Physica E 42 (2010) 2391–2401

Contents lists available at ScienceDirect

Physica E

journal homepage: www.elsevier.com/locate/physe

Longitudinal and transverse vibration of a single-walled carbon nanotube subjected to a moving nanoparticle accounting for both nonlocal and inertial effects

Keivan Kiani *

Department of Civil Engineering, Sharif University of Technology, Azadi Ave., P.O. Box 11365-9313, Tehran, Iran

ARTICLE INFO

Article history:
Received 29 April 2010
Received in revised form
18 May 2010
Accepted 19 May 2010
Available online 26 May 2010

Keywords:
Single-walled carbon nanotubes (SWCNTs)
Moving nanoparticle
Inertial effects
Nonlocal Rayleigh beam theory

ABSTRACT

Single-walled carbon nanotubes (SWCNTs) can be promising delivery nanodevices for a diverse range of applications, however, little is known about their dynamical interactions with moving nanoscale particles. In this paper, dynamic response of a SWCNT subjected to a moving nanoparticle is examined in the framework of the nonlocal continuum theory of Eringen. The inertial effects of the moving nanoparticle and the existing friction between the nanoparticle surface and the inner surface of the SWCNT are incorporated in the formulation of the problem. The equivalent continuum structure associated with the SWCNT is considered and modeled using nonlocal Rayleigh beam theory under simply supported boundary conditions. The governing equations are then established both in the strong and weak forms. The set of linear equations are solved in the time domain using generalized Newmark-β method. The effects of mass weight of the moving nanoparticle, its velocity, and small scale effect parameter on the dynamic amplitude factors of longitudinal and transverse displacements as well as those of axial force and bending moment are studied in some detail. Additionally, the possibility of moving nanoparticle separation from the inner surface of the SWCNT is investigated. The role of influential parameters on the possibility of this phenomenon is also addressed and discussed.

1. Introduction

In a lecture in 1959, the well-known physicist Feynman predicted the outlook of innovations in nanoscale sciences [1], now called nanotechnology. It was stipulated that this new field of physics will make to enable humankind to construct much smaller timesaving devices. It was emphasized that this fact would not be unexpected if humankind could find appropriate ways to manipulate and control things at the atomistic scale. In the aforementioned lecture, Feynman expressed that there is plenty of room at the bottom. It does imply that there is a room that you can decrease the size of things in a practical way. Perhaps it can be said that one of the above-mentioned rooms was found when Iijima [2] discovered carbon nanotubes (CNTs) in 1991. Just a short time after that, a large body of theoretical and experimental works was conducted to investigate the mechanical behavior of CNTs. The astonishing properties of CNTs make them as a promising technology for potential applications. The newly produced materials have extremely high strength, nearly perfect geometrical structure, low mass density, and linear elastic behavior for longitudinal strain lower than 12%. These extraordinary properties of CNTs provide them in many applications in nanotechnology, nanobiology, optic, electronic, and other fields of material sciences as well as in medical fields. Within the aforementioned fields of applications for CNTs, one use of CNTs is as new transporter systems for the delivery of drugs [3–6]. In such a case, one confronts the problem of interaction between CNTs and moving nanoscale objects.

When a nanoparticle starts to move inside a single-walled carbon nanotube (SWCNT), the SWCNT generally vibrates in the transverse and longitudinal directions due to the mass weight of the moving nanoparticle and the existing friction between the outer surface of the moving nanoparticle and the inner surface of the SWCNT. When the mass weight of the moving nanoparticle is negligible in comparison with the mass weight of the SWCNT, the inertial effects of the moving nanoparticle are insignificant. For this case, vibration of a nanotube structure under a moving nanoparticle was examined by Kiani and Mehri [7] using nonlocal beam theories. The explicit expressions of dynamical deflection and angle of rotation fields for each nonlocal beam were obtained. Moreover, the critical velocity of the moving nanoparticle was evaluated for each nonlocal beam model in the context of nonlocal continuum theory of Eringen. In another study, Kiani [8,9] investigated the dynamic behavior of double-walled carbon

* Tel.: +98 21 66164264; fax: +98 21 66014828.
E-mail addresses: k_kiani@civil.sharif.edu, keivankiani@yahoo.com.

1386-9477/$ - see front matter © 2010 Elsevier B.V. All rights reserved.
doi:10.1016/j.physe.2010.05.021

nanotubes (DWCNTs) traversed by a moving nanoparticle by employing various nonlocal beam models. In the studied problem, it was presumed that the inertial effects of the moving nanoparticle would be infinitesimal. The explicit expressions of dynamic displacements of both the innermost and outermost CNTs are then extracted by considering the existing van-der-Waals forces between the layers of CNTs. Additionally, the critical velocities of the moving nanoparticle for various models are established and the role of important parameters on the critical velocities was addressed and discussed in some detail. However, as the mass weight of the moving nanoparticle increases, its inertial effects could not be ignored at all. In contrast to the previous case, the linear relationship between the maximum dynamic deflection and the mass weight of the moving nanoparticle would be no longer valid. Furthermore, due to entrance of the inertial effects in the equations of motion, seeking an exact solution for the problem is fairly impossible. In such a case, the proper consideration of the inertial effects of the moving nanoparticle plays an important role in rational prediction of dynamic response of the SWCNTs. For this purpose, special treatments should be taken into account for solving of the problem.

In the problems of interaction of a SWCNT with a moving nanoparticle, the wavelength of the propagated sound waves through the SWCNT is strongly depended on the mass weight and velocity of the moving nanoparticle as well as material properties, geometry and boundary conditions of the SWCNT. On the other hand, as the wavelength becomes comparable to the length of the SWCNT, the application of the classical continuum theory would be doubtful since it cannot reasonably predict the dynamic response of the nanostructure [10]. To overcome this drawback of the classical continuum theory, the nonlocal continuum theory of Eringen [10,11] is exploited in the present work. The so-called continuum theory states that the stress at each point of the medium is also affected by the stresses at the neighboring points of that point. Such affectivity is described by an appropriate kernel function accounting for the internal atomistic length. Up to now, the nonlocal continuum theory of Eringen has been adopted for various types of problems associated with the SWCNTs, including buckling [12–14], postbuckling [15], linear free vibration [16–18] and nonlinear free vibration of the SWCNTs [19].

This paper deals with the dynamic response of a SWCNT under a moving nanoparticle based on the nonlocal Rayleigh beam theory (NRBT). The full inertial terms of the moving nanoparticle associated with the longitudinal and transverse vibration of the SWCNT as well as its friction with the inner surface of the SWCNT are incorporated in the theoretical formulations of the problem. The discrete equations of motion are obtained and then appropriately solved. The effects of moving nanoparticle velocity, mass weight of the moving nanoparticle, and small scale effect parameter on the dynamic amplitude factors of longitudinal and transverse displacements as well as those of axial force and bending moment are examined in some detail. The possibility of moving nanoparticle separation from the inner surface of the SWCNT is also explored. The role of influential parameters on the possibility of this phenomenon is then addressed and discussed.

2. Modeling of the problem

2.1. Description of the mathematical model

Dynamic analysis of a SWCNT under a moving nanomass using molecular mechanics would be a difficult job. It is because of the fact that most of the terms associated with the sum of the potentials of all atoms should be modified at each time step of calculations. Therefore, the computational effort for solving the problem dramatically increases. For convenience in vibration analysis of SWCNTs, some useful equivalent continuum structures (ECSs) have been developed [20–22]. In the suggested models, the ECS is often a homogeneous isotropic cylinder with the length and the mean radius equal to those of the SWCNT. The thickness of the ECS is then obtained such that its frequencies for the desired vibration modes or its displacements would be identical to those of the SWCNT with a good accuracy.

Now consider an ECS corresponding to a SWCNT of length l_b, cross-sectional area A_b, cross-sectional inertia moment I_b, Young's modulus E_b, and density ρ_b, as shown in Fig. 1. The simply supported ECS is axially pinned at its left end and movable at its right end. The longitudinal and transverse displacement fields of the ECS is denoted by $u(x,t)$ and $w(x,t)$, respectively. The ECS is acted upon by a moving nanoparticle of mass M and constant velocity v. The moving nanoparticle would be in contact with the ECS when it travels inside the ECS. The existing friction between the outer surface of the moving nanoparticle and inner surface of the ECS is simulated using the Coulomb friction model. However, the author knows that the friction at the nanoscale would be more complex than the assumed model. Since this issue has not been completely understood until now, we use this simple model to investigate the effect of the friction on the coupling between the longitudinal and transverse displacements. It is assumed that the ratio of the length to the diameter of the ECS is generally as great as that the predicted results by the NRBT would be trustable [7].

2.2. Equations of motion in the context of nonlocal continuum mechanics

The equations of motion in the context of nonlocal continuum theory based on the Rayleigh beam theory could be expressed as

$$\rho_b A_b \ddot{u} - N^{nl}_{b,x} = M\left(\mu_x\left|g-\frac{D^2w}{Dt^2}\right|-\frac{D^2u}{Dt^2}\right)\delta(x-x_M)H(l_b-x_M), \tag{1a}$$

$$\rho_b(A_b\ddot{w}-I_b\ddot{w}_{,xx})-M^{nl}_{b,xx} = M\left(g-\frac{D^2w}{Dt^2}\right)\delta(x-x_M)H(l_b-x_M), \tag{1b}$$

where g is the applied gravitational acceleration, μ_x is the coefficient of kinetic friction, x_M is the location of the moving nanoparticle ($x_M=vt$), H is the Heaviside step function, δ is the Dirac delta function. Moreover, $\dot{(\cdot)}$ and D represent the time and material derivatives, respectively. Based on the nonlocal continuum mechanics of Eringen, the nonlocal axial force (N^{nl}_b) and the nonlocal bending moment (M^{nl}_b) within the ECS are provided by

$$N^{nl}_b-(e_0a)^2N^{nl}_{b,xx} = E_bA_bu_{,x}, \tag{2a}$$

$$M^{nl}_b-(e_0a)^2M^{nl}_{b,xx} = -E_bI_bw_{,xx}, \tag{2b}$$

where e_0a is the small scale effect parameter. The value of this parameter could be determined by justification of the obtained results by the nonlocal continuum theory with those of atomistic-based models. Using Eqs. (1) and (2), the nonlocal axial force and bending moment in terms of displacements are obtained in the

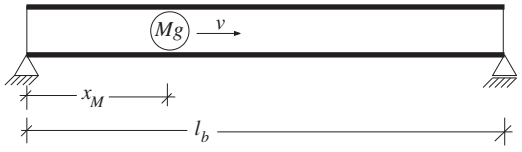

Fig. 1. A simply supported SWCNT subjected to a moving nanoparticle.

following form:

$$N_b^{nl}=E_bA_bu_{,x}+(e_0a)^2\left[\rho_bA_b\ddot{u}-M\left(\mu_x\left|g-\frac{D^2w}{Dt^2}\right|-\frac{D^2u}{Dt^2}\right)\delta(x-x_M)H(l_b-x_M)\right]_{,x}, \tag{3a}$$

$$M_b^{nl}=-E_bI_bw_{,xx}+(e_0a)^2\left[\rho_b(A_b\ddot{w}-I_b\ddot{w}_{,xx})-M\left(g-\frac{D^2w}{Dt^2}\right)\delta(x-x_M)H(l_b-x_M)\right], \tag{3b}$$

substituting Eq. (3) into Eq. (1) gives the governing equations as follows:

$$\rho_bA_b(\ddot{u}-(e_0a)^2\ddot{u}_{,xx})-E_bA_bu_{,xx}=M\left[\left(\mu_x\left|g-\frac{D^2w}{Dt^2}\right|-\frac{D^2u}{Dt^2}\right)\delta(x-x_M)-(e_0a)^2\left(\left(\mu_x\left|g-\frac{D^2w}{Dt^2}\right|-\frac{D^2u}{Dt^2}\right)\delta(x-x_M)\right)_{,xx}\right]H(l_b-x_M), \tag{4a}$$

$$\rho_b(A_b\ddot{w}-I_b\ddot{w}_{,xx})-(e_0a)^2\rho_b(A_b\ddot{w}_{,xx}-I_b\ddot{w}_{,xxxx})+E_bI_bw_{,xxxx}=M\left[\left(g-\frac{D^2w}{Dt^2}\right)\delta(x-x_M)-(e_0a)^2\left(\left(g-\frac{D^2w}{Dt^2}\right)\delta(x-x_M)\right)_{,xx}\right]H(l_b-x_M). \tag{4b}$$

Eqs. (4a) and (4b) represent the strong form of the equations of motion for a SWCNT under a moving nanoparticle by considering the frictional and inertial effects of the moving nanoparticle. If the value of small scale effect parameter is set equal to zero, one could arrive at the equations of motion of a macroscale beam under a moving mass.

3. Solving the governing equations

Generally, finding an analytical solution to Eq. (4) is so difficult due to the presence of the first spatial differentiation of the displacements in the right hand side of Eqs. (4a) and (4b). As a result, finding a suitable numerical approach to solve the problem would be of great advantage. In this paper, the unknown displacements are discretized in terms of mode shapes associated with the boundary conditions of the problem. To construct the discrete form of the governing equations, both sides of Eqs. (4a) and (4b) are, respectively, multiplied by δu and δw. Subsequently, by integration over the length of the nanotube structure and application of the integration by parts

$$\int_0^{l_b}\left\{\rho_bA_b\delta w\ddot{w}+\rho_bI_b\delta w_{,x}\ddot{w}_{,x}+E_bI_b\delta w_{,xx}w_{,xx}-\delta wM\left(g-\frac{D^2w}{Dt^2}\right)\delta(x-x_M)H(l_b-x_M)-(e_0a)^2\delta w_{,xx}\left(\rho_b\left(A_b\ddot{w}-I_b\ddot{w}_{,xx}\right)-M\left(g-\frac{D^2w}{Dt^2}\right)\delta(x-x_M)H(l_b-x_M)\right)+\rho_bA_b\delta u\ddot{u}+E_bA_b\delta u_{,x}u_{,x}-M\left(\mu_x\left|g-\frac{D^2w}{Dt^2}\right|-\frac{D^2u}{Dt^2}\right)\delta u\delta(x-x_M)H(l_b-x_M)+(e_0a)^2\left(\rho_bA_b\delta u_{,x}\ddot{u}_{,x}-M\delta u_{,x}\left(\left(\mu_x\left|g-\frac{D^2w}{Dt^2}\right|-\frac{D^2u}{Dt^2}\right)\times\delta(x-x_M)\right)_{,x}H(l_b-x_M)\right)\right\}dx=0. \tag{5}$$

The displacement field of the problem are expressed in terms of mode shapes as

$$u(x,t)=\sum_{i=1}^{nm}\phi_i^u(x)u_i(t), \tag{6a}$$

$$w(x,t)=\sum_{i=1}^{nm}\phi_i^w(x)w_i(t), \tag{6b}$$

where $\phi_i^u(x)$ and $\phi_i^w(x)$ are, respectively, the ith mode shapes associated with the longitudinal and transverse displacements, $u_i(t)$ and $w_i(t)$ are the unknown coefficients pertinent to the ith mode shapes of displacements, and nm is the number of modes required for appropriate discretization of the displacement fields. Substitution of Eq. (6) into Eq. (5) would result in the following discrete form of the governing equations

$$\begin{bmatrix}[\mathbf{M}_b]^{uu} & [\mathbf{M}_b]^{uw}\\ [\mathbf{M}_b]^{wu} & [\mathbf{M}_b]^{ww}\end{bmatrix}\begin{Bmatrix}\ddot{\mathbf{u}}\\ \ddot{\mathbf{w}}\end{Bmatrix}+\begin{bmatrix}[\mathbf{C}_b]^{uu} & [\mathbf{C}_b]^{uw}\\ [\mathbf{C}_b]^{wu} & [\mathbf{C}_b]^{ww}\end{bmatrix}\begin{Bmatrix}\dot{\mathbf{u}}\\ \dot{\mathbf{w}}\end{Bmatrix}+\begin{bmatrix}[\mathbf{K}_b]^{uu} & [\mathbf{K}_b]^{uw}\\ [\mathbf{K}_b]^{wu} & [\mathbf{K}_b]^{ww}\end{bmatrix}\begin{Bmatrix}\mathbf{u}\\ \mathbf{w}\end{Bmatrix}=\begin{Bmatrix}\{\mathbf{f}_b\}^u\\ \{\mathbf{f}_b\}^w\end{Bmatrix}, \tag{7}$$

where

$$[\mathbf{M}_b]_{ij}^{uu}=\int_0^{l_b}\rho_bA_b(\phi_i^u\phi_j^u+(e_0a)^2\phi_{i,x}^u\phi_{j,x}^u)\,dx+M(\phi_i^u(x_M)-(e_0a)^2\phi_{i,xx}^u(x_M))\phi_j^u(x_M)H(l_b-x_M), \tag{8a}$$

$$[\mathbf{M}_b]_{ij}^{uw}=\mu_xM\,\mathrm{sgn}\left(g-\frac{D^2w(x_M,t)}{Dt^2}\right)(\phi_i^u(x_M)-(e_0a)^2\phi_{i,xx}^u(x_M))\phi_j^w(x_M)H(l_b-x_M), \tag{8b}$$

$$[\mathbf{M}_b]_{ij}^{ww}=\int_0^{l_b}[\rho_b(A_b\phi_i^w\phi_j^w+I_b\phi_{i,x}^w\phi_{j,x}^w)-(e_0a)^2\rho_b\phi_{i,xx}^w(A_b\phi_j^w-I_b\phi_{j,xx}^w)]\,dx+M(\phi_i^w(x_M)-(e_0a)^2\phi_{i,xx}^w(x_M))\phi_j^w(x_M)H(l_b-x_M), \tag{8c}$$

$$[\mathbf{C}_b]_{ij}^{uu}=2M\nu(\phi_i^u(x_M)-(e_0a)^2\phi_{i,xx}^u(x_M))\phi_{j,x}^u(x_M)H(l_b-x_M), \tag{8d}$$

$$[\mathbf{C}_b]_{ij}^{uw}=2\mu_xM\nu\,\mathrm{sgn}\left(g-\frac{D^2w(x_M,t)}{Dt^2}\right)(\phi_i^u(x_M)-(e_0a)^2\phi_{i,xx}^u(x_M))\phi_{j,x}^w(x_M)H(l_b-x_M), \tag{8e}$$

$$[\mathbf{C}_b]_{ij}^{ww}=2M\nu(\phi_i^w(x_M)-(e_0a)^2\phi_{i,xx}^w(x_M))\phi_{j,x}^w(x_M)H(l_b-x_M), \tag{8f}$$

$$[\mathbf{K}_b]_{ij}^{uu}=\int_0^{l_b}E_bA_b\phi_{i,x}^u\phi_{j,x}^u\,dx+M\nu^2(\phi_i^u(x_M)-(e_0a)^2\phi_{i,xx}^u(x_M))\phi_{j,xx}^u(x_M)H(l_b-x_M), \tag{8g}$$

$$[\mathbf{K}_b]_{ij}^{uw}=\mu_xM\nu^2\,\mathrm{sgn}\left(g-\frac{D^2w(x_M,t)}{Dt^2}\right)(\phi_i^u(x_M)-(e_0a)^2\phi_{i,xx}^u(x_M))\phi_{j,xx}^w(x_M)H(l_b-x_M), \tag{8h}$$

$$[\mathbf{K}_b]_{ij}^{ww}=\int_0^{l_b}E_bI_b\phi_{i,xx}^w\phi_{j,xx}^w\,dx+M\nu^2(\phi_i^w(x_M)-(e_0a)^2\phi_{i,xx}^w(x_M))\phi_{j,xx}^w(x_M)H(l_b-x_M), \tag{8i}$$

$$\{\mathbf{f}_b\}_i^u=\mu_xMg\,\mathrm{sgn}\left(g-\frac{D^2w(x_M,t)}{Dt^2}\right)(\phi_i^u(x_M)-(e_0a)^2\phi_{i,xx}^u(x_M))H(l_b-x_M), \tag{8j}$$

$$\{\mathbf{f}_b\}_i^w=Mg(\phi_i^w(x_M)-(e_0a)^2\phi_{i,xx}^w(x_M))H(l_b-x_M), \tag{8k}$$

by introducing the following dimensionless parameters

$$\xi=\frac{x}{l_b},\quad \overline{u}=\frac{u}{l_b},\quad \overline{w}=\frac{w}{l_b},\quad \tau=\frac{1}{l_b^2}\sqrt{\frac{E_bI_b}{\rho_bA_b}}t,\quad \mu=\frac{e_0a}{l_b},$$

$$\lambda=\frac{l_b}{r_b},\quad C_L=\sqrt{\frac{E_b}{\rho_b}},\quad M_N=\frac{M}{\rho_bA_bl_b},\quad \beta=\frac{\nu}{C_L},\quad \gamma=\frac{\sqrt{gl_b}}{C_L}. \tag{9}$$

Eq. (7) could be rewritten in the dimensionless form as

$$\begin{bmatrix} [\overline{\mathbf{M}}_b]^{uu} & [\overline{\mathbf{M}}_b]^{uw} \\ [\overline{\mathbf{M}}_b]^{wu} & [\overline{\mathbf{M}}_b]^{ww} \end{bmatrix} \begin{Bmatrix} \overline{\mathbf{u}}_{,\tau\tau} \\ \overline{\mathbf{w}}_{,\tau\tau} \end{Bmatrix} + \begin{bmatrix} [\overline{\mathbf{C}}_b]^{uu} & [\overline{\mathbf{C}}_b]^{uw} \\ [\overline{\mathbf{C}}_b]^{wu} & [\overline{\mathbf{C}}_b]^{ww} \end{bmatrix} \begin{Bmatrix} \overline{\mathbf{u}}_{,\tau} \\ \overline{\mathbf{w}}_{,\tau} \end{Bmatrix} + \begin{bmatrix} [\overline{\mathbf{K}}_b]^{uu} & [\overline{\mathbf{K}}_b]^{uw} \\ [\overline{\mathbf{K}}_b]^{wu} & [\overline{\mathbf{K}}_b]^{ww} \end{bmatrix} \begin{Bmatrix} \overline{\mathbf{u}} \\ \overline{\mathbf{w}} \end{Bmatrix} = \begin{Bmatrix} \{\overline{\mathbf{f}}_b\}^u \\ \{\overline{\mathbf{f}}_b\}^w \end{Bmatrix}, \tag{10}$$

where the nonzero nondimensional submatrices are stated as

$$[\overline{\mathbf{M}}_b]_{ij}^{uu} = \int_0^1 (\phi_i^u \phi_j^u + \mu^2 \phi_{i,\xi}^u \phi_{j,\xi}^u)\, d\xi + M_N(\phi_i^u(\xi_M) - \mu^2 \phi_{i,\xi\xi}^u(\xi_M))\phi_j^u(\xi_M) H(1-\xi_M), \tag{11a}$$

$$[\overline{\mathbf{M}}_b]_{ij}^{uw} = \mu_x M_N \operatorname{sgn}\left(1-\left(\frac{1}{\lambda\gamma}\right)^2 \diamond \overline{w}(\xi_M,\tau)\right)(\phi_i^u(\xi_M) - \mu^2 \phi_{i,\xi\xi}^u(\xi_M))\phi_j^w(\xi_M) H(1-\xi_M), \tag{11b}$$

$$[\overline{\mathbf{M}}_b]_{ij}^{ww} = \int_0^1 [(\phi_i^w \phi_j^w + \lambda^{-2}\phi_{i,\xi}^w \phi_{j,\xi}^w) - \mu^2 \phi_{i,\xi\xi}^w(\phi_j^w - \lambda^{-2}\phi_{j,\xi\xi}^w)]\, d\xi + M_N(\phi_i^w(\xi_M) - \mu^2 \phi_{i,\xi\xi}^w(\xi_M))\phi_j^w(\xi_M) H(1-\xi_M), \tag{11c}$$

$$[\overline{\mathbf{C}}_b]_{ij}^{uu} = 2\lambda\beta M_N(\phi_i^u(\xi_M) - \mu^2 \phi_{i,\xi\xi}^u(\xi_M))\phi_{j,\xi}^u(\xi_M) H(1-\xi_M), \tag{11d}$$

$$[\overline{\mathbf{C}}_b]_{ij}^{uw} = 2\mu_x\lambda\beta M_N \operatorname{sgn}\left(1-\left(\frac{1}{\lambda\gamma}\right)^2 \diamond \overline{w}(\xi_M,\tau)\right)(\phi_i^u(\xi_M) - \mu^2 \phi_{i,\xi\xi}^u(\xi_M))\phi_{j,\xi}^w(\xi_M) H(1-\xi_M), \tag{11e}$$

$$[\overline{\mathbf{C}}_b]_{ij}^{ww} = 2\lambda\beta M_N(\phi_i^w(\xi_M) - \mu^2 \phi_{i,\xi\xi}^w(\xi_M))\phi_{j,\xi}^w(\xi_M) H(1-\xi_M), \tag{11f}$$

$$[\overline{\mathbf{K}}_b]_{ij}^{uu} = \lambda^2 \int_0^1 \phi_{i,\xi}^u \phi_{j,\xi}^u\, d\xi + M_N(\lambda\beta)^2(\phi_i^u(\xi_M) - \mu^2 \phi_{i,\xi\xi}^u(\xi_M))\phi_{j,\xi\xi}^u(\xi_M) H(1-\xi_M), \tag{11g}$$

$$[\overline{\mathbf{K}}_b]_{ij}^{uw} = \mu_x(\lambda\beta)^2 M_N \operatorname{sgn}\left(1-\left(\frac{1}{\lambda\gamma}\right)^2 \diamond \overline{w}(\xi_M,\tau)\right)(\phi_i^u(\xi_M) - \mu^2 \phi_{i,\xi\xi}^u(\xi_M))\phi_{j,\xi\xi}^w(\xi_M) H(1-\xi_M), \tag{11h}$$

$$[\overline{\mathbf{K}}_b]_{ij}^{ww} = \int_0^1 \phi_{i,\xi\xi}^w \phi_{j,\xi\xi}^w\, d\xi + M_N(\lambda\beta)^2(\phi_i^w(\xi_M) - \mu^2 \phi_{i,\xi\xi}^w(\xi_M))\phi_{j,\xi\xi}^w(\xi_M) H(1-\xi_M), \tag{11i}$$

$$\{\overline{\mathbf{f}}_b\}_i^u = \mu_x(\lambda\gamma)^2 M_N \operatorname{sgn}\left(1-\left(\frac{1}{\lambda\gamma}\right)^2 \diamond \overline{w}(\xi_M,\tau)\right)(\phi_i^u(\xi_M) - \mu^2 \phi_{i,\xi\xi}^u(\xi_M)) H(1-\xi_M), \tag{11j}$$

$$\{\overline{\mathbf{f}}_b\}_i^w = (\lambda\gamma)^2 M_N(\phi_i^w(\xi_M) - \mu^2 \phi_{i,\xi\xi}^w(\xi_M)) H(1-\xi_M), \tag{11k}$$

in which in Eq. (11), the operator $\diamond$ is defined as

$$\diamond \overline{w} = \left(\frac{\partial}{\partial\tau} + \lambda\beta\frac{\partial}{\partial\xi}\right)\left(\frac{\partial \overline{w}}{\partial\tau} + \lambda\beta\frac{\partial \overline{w}}{\partial\xi}\right), \tag{12}$$

the nonlocal axial force and bending moment within the ECS in terms of nondimensional displacement components are expressed as follows:

$$N_b^{nl} = E_b A_b \left\{ \overline{u}_{,\xi} + \mu^2 \left[\frac{1}{\lambda^2}\overline{u}_{,\tau\tau\xi} - \mu_x M_N \gamma^2 \operatorname{sgn}\left(1-\left(\frac{1}{\lambda\gamma}\right)^2 \diamond \overline{w}(\xi_M,\tau)\right) \times \left(\left(1-\left(\frac{1}{\lambda\gamma}\right)^2 \diamond \overline{w}(\xi_M,\tau)\right)\delta(\xi-\xi_M)\right)_{,\xi} H(1-\xi_M) \right] \right\}, \tag{13a}$$

$$M_b^{nl} = \frac{E_b I_b}{l_b} \left\{ -\overline{w}_{,\xi\xi} + \mu^2 \left[\overline{w}_{,\tau\tau} - \frac{1}{\lambda^2}\overline{w}_{,\tau\tau\xi\xi} - M_N(\lambda\gamma)^2 \left(1-\left(\frac{1}{\lambda\gamma}\right)^2 \diamond \overline{w}\right) \times \delta(\xi-\xi_M) H(1-\xi_M) \right] \right\}. \tag{13b}$$

Since study of the problem for a pinned-movable SWCNT under simply supported boundary conditions is of concern, the following normalized mode shapes should be taken into account (see Fig. 1)

$$\phi_i^u(\xi) = \sqrt{2}\sin((i-0.5)\pi\xi), \quad \phi_i^w(\xi) = \sqrt{2}\sin(i\pi\xi), \tag{14}$$

substitution of Eq. (14) into Eq. (11) and evaluation of the integrals, leads to the more simple expressions for the submatrices with integrals. The explicitly obtained statements for such submatrices are provided in Appendix. A. To solve the set of ordinary differential equations in Eq. (10) in the time domain, the generalized Newmark-β method is employed. This newly developed scheme has been explained in some detail in Ref. [23].

4. Results and discussions

4.1. Some comparisons

In this part, some comparisons are provided to ensure us about the accuracy of the presented model and calculations. For this purpose, the analytical expressions of the phase velocities associated with the longitudinally and transversely propagated waves are obtained and the results are compared with those of other researchers. Then, the plots of dynamic transverse displacement of the ECS under a moving nanoparticle will be presented. In a special case, the predicted results by the proposed model are also compared with those of another work.

4.1.1. Longitudinal and transverse wave propagation in the SWCNT

When the mass weight of the moving nanoparticle is negligible with respect to the mass weight of the SWCNT (i.e., $M_N=0$), the governing equations associated with the longitudinal and transverse vibrations are decouple. If one assume $\overline{u} = \overline{u}_0 e^{i\varpi_l \tau}$ and $\overline{w} = \overline{w}_0 e^{i\varpi_t \tau}$, Eq. (11) is then reduced to the following form

$$\det[-\varpi_l^2(\Upsilon_{ij}^{uu} + \mu^2 \Gamma_{ij}^{uu}) + \lambda^2 \Gamma_{ij}^{uu}] = 0, \tag{15a}$$

$$\det[-\varpi_t^2(\Upsilon_{ij}^{ww} + \lambda^{-2}\Gamma_{ij}^{ww} + \mu^2(\Xi_{ij}^{ww} + \lambda^{-2}\Sigma_{ij}^{ww})) + \Sigma_{ij}^{ww}] = 0, \tag{15b}$$

where ϖ_l and ϖ_t are, respectively, the dimensionless frequencies of the longitudinal and flexural waves. $\overline{u}_0$ and $\overline{w}_0$ in order are the initial values of the dimensionless longitudinal and transverse displacements. By solving the set of eigenvalue equations in Eq. (15) and using Eq. (A2), the eigenvalues (i.e., dimensionless natural frequencies) of the ECS modeled by the NRBT are obtained as

$$\varpi_{l_i} = \sqrt{\frac{\pi^2\lambda^2(i-0.5)i}{1+\pi^2\mu^2(i-0.5)i}}, \tag{16a}$$

$$\varpi_{t_i} = \sqrt{\frac{\pi^4 i^4}{1+\pi^4\mu^2\lambda^{-2}i^4 + \pi^2 i^2(\lambda^{-2}+\mu^2)}}. \tag{16b}$$

The phase velocities are defined as $v_{[]} = \omega_{[]}/k_{[]}; [] = l$ or t where $\varpi_{[]} = l_b^2\sqrt{\rho_b A_b/(E_b I_b)}\omega_{[]}$. The longitudinal and transverse wave numbers associated with the ith vibration modes of the under study ECS are readily expressed by $k_{l_i} = (i-0.5)\pi/l_b$ and $k_{t_i} = i\pi/l_b$, respectively. As a result, the explicit statements of longitudinal and transverse wave velocities of the ECS based on the NRBT are

derived as

$$v_{l_i} = \sqrt{\frac{E_b}{\rho_b}}\sqrt{\frac{i}{(1+\pi^2\mu^2(i-0.5)i)(i-0.5)}}, \tag{17a}$$

$$v_{t_i} = \frac{\pi i}{\lambda}\sqrt{\frac{E_b}{\rho_b}}\sqrt{\frac{1}{(1+\pi^2\mu^2 i^2)(1+\pi^2 i^2\lambda^{-2})}}, \tag{17b}$$

if the rotary inertia of the nonlocal beam is neglected, the term $1+\pi^2 i^2\lambda^{-2}$ is omitted in Eq. (17a). In such a case, one could arrive at the common expression of the flexural phase velocity for SWCNTs based on the nonlocal Euler–Bernoulli beam theory (NEBT) [24]

$$v_{t_i} = \frac{\pi i}{\lambda}\sqrt{\frac{E_b}{\rho_b}}\sqrt{\frac{1}{1+\pi^2\mu^2 i^2}}. \tag{18}$$

Comparison between Eqs. (17b) and (18) reveals that the predicted flexural phase velocities by the NRBT are always lower than those of the NEBT. Nevertheless, the differences between the phase velocities of the NRBT and the NEBT reduce with the slenderness ratio of the ECS.

4.1.2. Time history plots of the transverse displacement of the SWCNT

The time history plots of the normalized transverse displacement (w_N) of the midspan point of the ECS correspond to the SWCNT under a moving nanoparticle are depicted in Fig. 2(a) and (b) where $w_N = \overline{w}/(Mgl_b^2/(48E_bI_b))$. The results have been provided for three levels of the mass weight of the moving nanoparticle (i.e., M_N=0.001, 0.2, and 0.4) as well as three values of the normalized small scale effect parameter (i.e., $\mu = 0$, 0.3, and 0.5). Moreover, the geometry and material properties of the SWCNT are identical to those of the nanotube structure mentioned in Ref. [7]. The other parameters are as $nm=10$, $\mu_x = 0.3$, $\lambda = 50$, $\tau_f = \sqrt{E_b/\rho_b}/(\lambda v)$, and $v = 0.7\pi\sqrt{E_b/\rho_b}/\lambda$. The predicted results by the NEBT from Ref. [7] are also presented in Fig. 2(a) for the above-mentioned values of μ. In Ref. [7], neither the inertial effects of the moving nanoparticle nor its frictional effects were considered in the modeling of the problem. Therefore, for an infinitesimal magnitude of the mass weight of the moving nanoparticle (i.e., M_N=0.001), it is expected that the present theory could also predict the results of the NEBT which are presented in Ref. [7]. As it is seen in Fig. 2(a), the obtained results by the present model are in good agreement with those of the NEBT which was developed by Kiani and Mehri [7]. As it is obvious from Fig. 3(a) to (c), the maximum values of the plots of w_N increase with the mass weight of the moving nanoparticle as well as the normalized small scale effect parameter.

4.2. Numerical studies

In order to realize the role of important parameters on the interaction between a moving nanoparticle and a SWCNT, some instructive parametric studies are carried out. In this regard, the effects of the velocity and mass weight of the moving nanoparticle as well as the small scale effect parameter on the dynamic response of SWCNTs are studied in some detail. For this purpose, the thickness, mean radii and length of the ECS are set equal to 0.34, 1, and 30 nm, respectively. The density and Young's modulus of the ECS are in order assumed to be 2500 kg/m^3 and 1 TPa. The normalized velocity parameter of the moving nanoparticle is defined as $V_N = v/v_{cr}$ where $v_{cr} = \pi C_L/\lambda$. The dynamic amplitude factor (DAF) of the deflection/bending moment of the ECS under a moving nanoparticle, i.e., DAF_w/DAF_M, is defined as the ratio of the maximum dynamic deflection/bending moment to the maximum static deflection/bending moment due to the applied weight of the moving nanoparticle at the midspan point of the ECS. Additionally, the DAF of the axial displacement/axial force, i.e., DAF_u/DAF_N, is defined as the ratio of the maximum dynamic axial displacement/axial force to the maximum statically axial displacement/axial force due to an axially applied force with magnitude $\mu_x Mg$ at the midspan point of the ECS.

From macroscopic point of view, coefficient of kinetic friction relies on various parameters such as temperature, speed, aging and

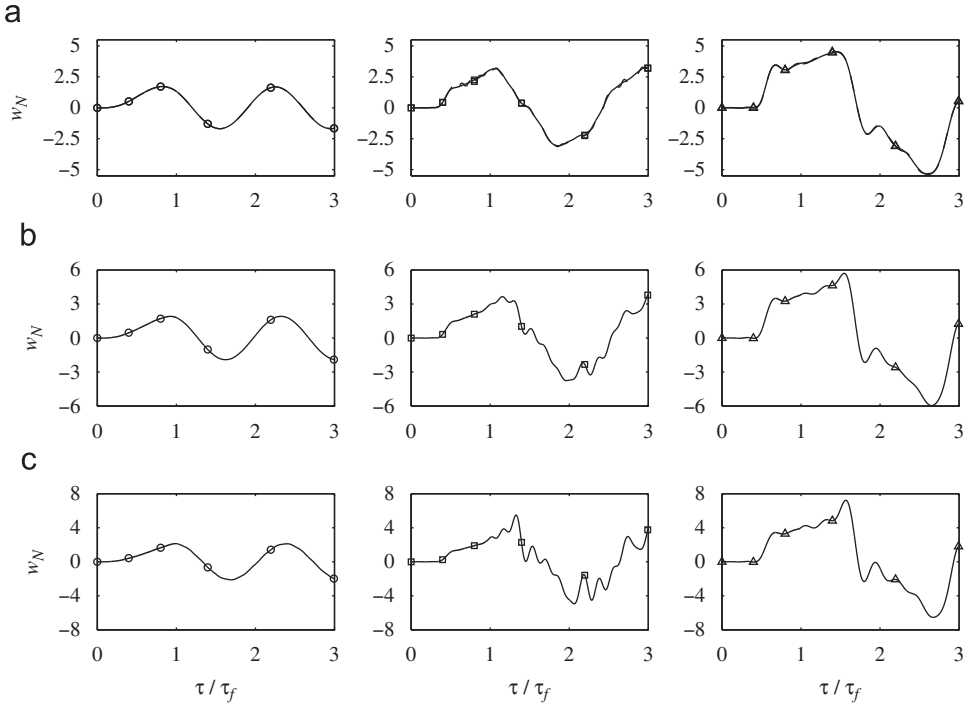

Fig. 2. Normalized dynamic transverse displacement at the midspan point of the ECS for various values of mass weight of the moving nanoparticle: (a) M_N=0.001, (b) M_N=0.2, and (c) M_N= 0.4 (○) $\mu = 0$; (□) $\mu = 0.3$; (△) $\mu = 0.5$; (– – –) Kiani and Mehri [7]; and (—) present work).

deaging times as well as the roughness of the pair of surfaces in contact. For macroscale structures, the coefficient of friction is determined empirically. For most dry surfaces of macroscale materials in contact, the coefficient of friction is commonly in the range of 0.3–0.6. On the other hand, determining the forces required to move an atom or a molecule over a set of them is a challenging issue in designing nanodevices. In 2008, Ternes et al. [25] could move a single atom on a surface for the first time, and the normal and lateral forces were measured. Using ultrahigh vacuum at the nearly zero Kelvin temperature, a modified atomic force microscope was utilized to force a cobalt atom, and a carbon monoxide molecule, across the surfaces of copper and platinum. It was found that the needed force for moving an atom on the surface depends robustly on the adsorbate and the surface. The obtained results also revealed that the lateral force plays the dominant role for moving the metal atoms on the metal surfaces. A brief survey of the literature reveals that there is a lack of sufficient information regarding the coefficient of kinetic friction in the atomic scale. As a result, its value for the Coulomb model is set equal to a low value of the coefficient of friction for macroscale materials, namely 0.3. However, it will be shown that the predicted DAFs of displacements as well as those of internal forces of the SWCNT do not vary with the coefficient of kinetic friction.

The value of the small scale effect parameter is determined by comparing the predicted dispersion curves by the nonlocal model with those obtained by an appropriate atomistic-based model. Through justification of the results of the higher order strain gradient for elastic beams with those of molecular dynamics, Wang and Hu [18] suggested $e_0=0.288$ for SWCNTs with armchair construction. Sudak [12] used $a=0.142$ nm for buckling analysis of multi-walled carbon nanotubes. In another study, Wang et al. [26] proposed a value of $e_0a=0.7$ nm for the application of the nonlocal elastic rod theory in prediction of axial stiffness of SWCNTs. The obtained results were compared with those of molecular dynamics and a good agreement was achieved. On the other hand, the nonlocal small scale parameter e_0a is generally considered in the range of 0–2 nm [27–30] for the dynamic analysis of CNTs. In the present work, the obtained results are presented for $e_0a=0$, 0.5, 1, and 1.5 nm.

Throughout this paper, the obtained results are demonstrated for two cases: without and with consideration of the inertial effects of the moving nanoparticle. The results of these cases are presented by dashed and solid lines, respectively. Moreover, the latter case describes the problem of moving nanoparticle–SWCNTs interaction and the differences between the results of these two cases show the effects of the moving nanoparticle inertia.

4.2.1. *The effect of the velocity of the moving nanoparticle on the DAFs of displacements and forces of the SWCNT*

The effect of the velocity of the moving nanoparticle on DAF_u, DAF_N, DAF_w, and DAF_M has been depicted in Figs. 3–6. The plotted results have been provided for three levels of the mass weight of the moving nanoparticle (i.e., $M_N=0.001$, 0.2, and 0.4) and four levels of the small scale effect parameter (i.e., $e_0a=0$, 0.5, 1, and 1.5 nm). In Fig. 3(a)–(c), the predicted DAF_u in terms of V_N has been demonstrated. In the case of $M_N=0.001$, the DAF_u commonly increases with V_N up to a certain value of the moving nanoparticle velocity ($V_N\approx0.95$), regardless of the value of the small scale effect parameter. As the mass weight of the moving nanoparticle increases, the peaks of DAF_u-V_N occur in lower levels of the velocity of the moving nanoparticle. For instant, the maximum of the graphs DAF_u-V_N for $M_N=0.2$ and 0.4 would take place in $V_N\approx0.77$ and 0.67, correspondingly. The magnitude of DAF_u increases with M_N, irrespective of the magnitude of e_0a. Moreover, the value of DAF_u would generally magnify with small scale effect parameter for most values of V_n, irrespective of M_N. The predicted values of DAF_w as a function of V_N are presented in Fig. 4(a)–(c). The differences between the predicted values of the above-mentioned two cases would generally increase with the mass weight of the moving nanoparticle, particularly for high levels of the velocity. Equally important, as the mass weight of the moving nanoparticle increases, the maximum of DAF_w occurs in higher values of velocity. For both cases, with and without considering the inertial effect, the predicted values of DAF_w would generally increase with the small scale effect parameter. The plots of DAF of axial force (DAF_N) in terms of V_N have been provided in

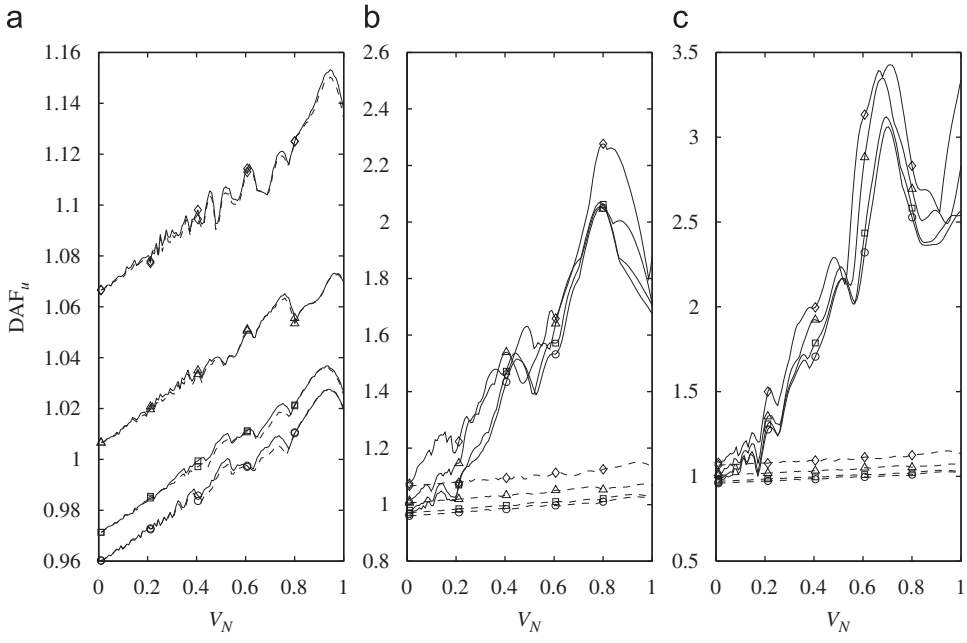

Fig. 3. Plots of DAF_u in terms of V_N: (a) $M_N=0.001$, (b) $M_N=0.2$, and (c) $M_N=0.4$ ((○) $e_0a=0$ nm; (□) $e_0a=0.5$ nm; (△) $e_0a=1$ nm; (◇) $e_0a=1.5$ nm; (– – –) without considering the inertial effects; and (—) by considering the inertial effects).

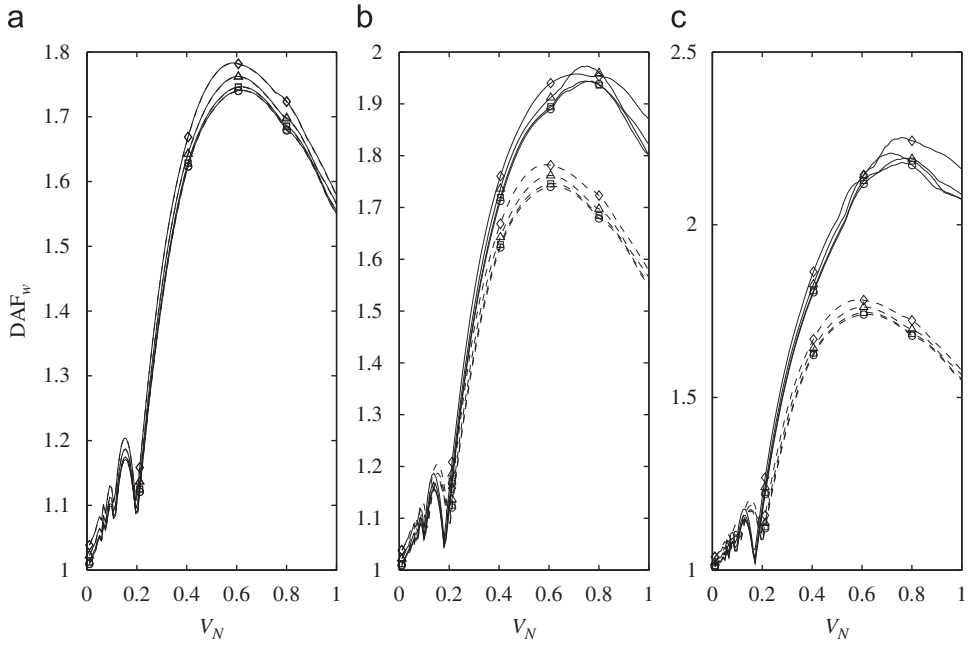

Fig. 4. Plots of DAF$_w$ in terms of V_N: (a) M_N=0.001, (b) M_N=0.2, and (c) M_N=0.4 ((◦) e_0a = 0 nm; (□) e_0a = 0.5 nm; (△) e_0a = 1 nm; (◇) e_0a = 1.5 nm; (– – –) without considering the inertial effects; and (—) by considering the inertial effects).

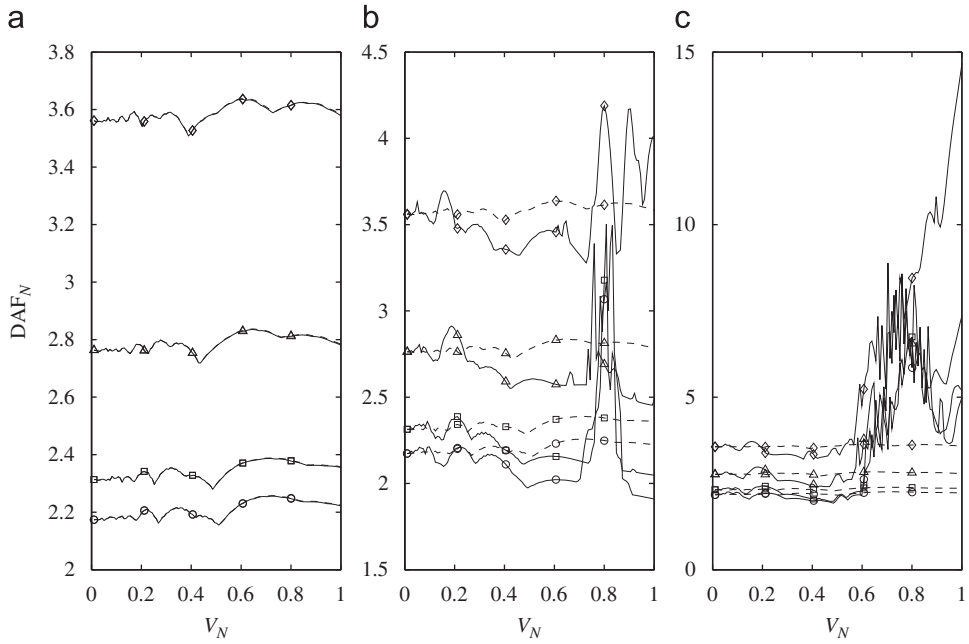

Fig. 5. Plots of DAF$_N$ in terms of V_N: (a) M_N=0.001, (b) M_N=0.2, and (c) M_N=0.4 ((◦) e_0a = 0 nm; (□) e_0a = 0.5 nm; (△) e_0a = 1 nm; (◇) e_0a = 1.5 nm; (– – –) without considering the inertial effects; and (—) by considering the inertial effects).

Fig. 5(a)–(c). In the case of M_N=0.001, DAF$_N$ varies slightly with V_N. As the mass weight of the moving nanoparticle magnifies, the predicted values of DAF$_N$ by considering the inertial effect would be generally lower than those without considering the inertial effect for velocities lower than a certain value. In such cases, the graphs of DAF$_N$-V_N fluctuate harshly for some ranges of velocity of the moving nanoparticle (see Fig. 5(b) and (c)). As it will be discussed in the next parts, the main reason of this fact is the change of the contact force sign from positive to negative. The graphs of DAF associated with the bending moment of the SWCNT (DAF$_M$) as a function of V$_N$ have been plotted in Fig. 6(a)–(c). As it is expected, the predicted values of DAF$_M$ in two cases, with and without considering the inertial effects, are corresponding to each other for M_N=0.001. As the magnitudes of mass weight and velocity of the moving nanoparticle increase, the effects of inertia of the moving nanoparticle become highlighted. The general trend of the plots of DAF$_M$-V_N is somehow analogous to those of DAF$_w$-V_N.

4.2.2. Possibility of the moving nanoparticle separation from the inner surface of the SWCNT

An important analysis is given for the role of the moving nanoparticle velocity on the minimum value of the transverse

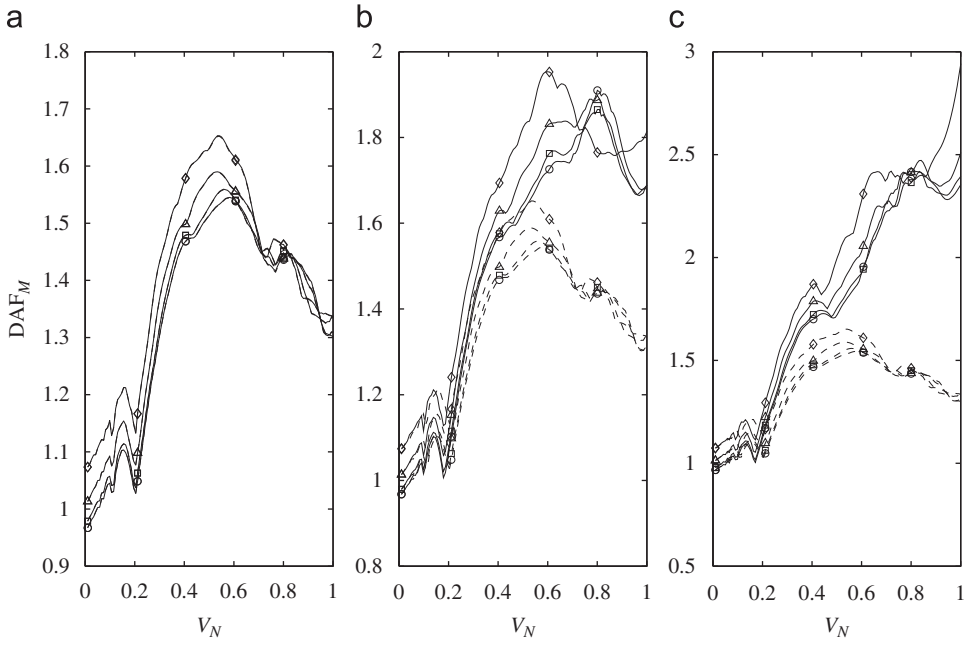

Fig. 6. Plots of DAF$_M$ in terms of V_N: (a) M_N=0.001, (b) M_N=0.2, and (c) M_N=0.4 ((○) $e_0a=0$ nm; (□) $e_0a=0.5$ nm; (△) $e_0a=1$ nm; (◇) $e_0a=1.5$ nm; (– – –) without considering the inertial effects; and (—) by considering the inertial effects).

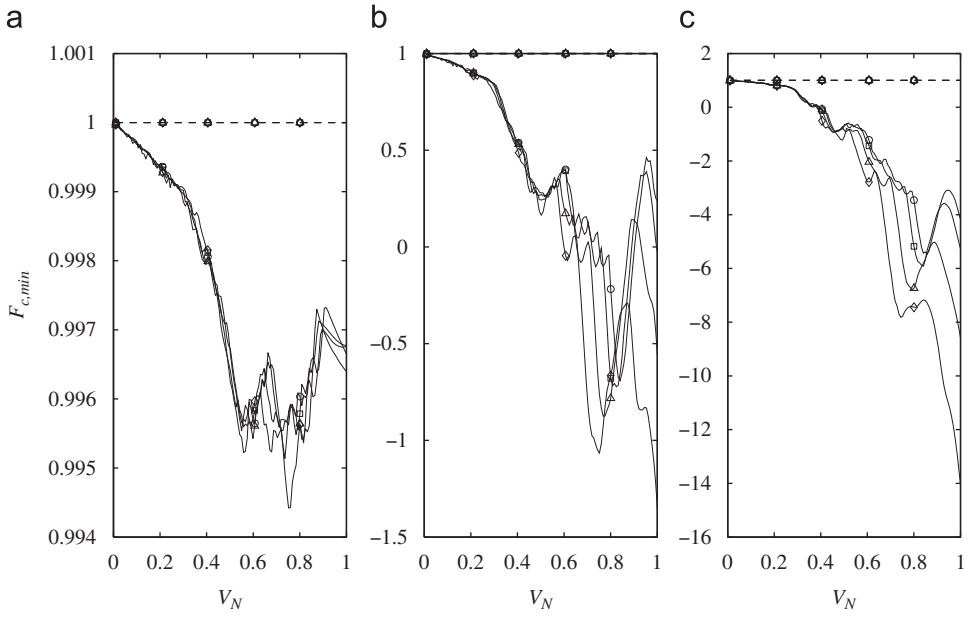

Fig. 7. Plots of $F_{c,\min}$ in terms of V_N: (a) M_N=0.001, (b) M_N=0.2, and (c) M_N=0.4 ((○) $e_0a=0$ nm; (□) $e_0a=0.5$ nm; (△) $e_0a=1$ nm; (◇) $e_0a=1.5$ nm; (– – –) without considering the inertial effects; and (—) by considering the inertial effects).

contact force for different values of the small scale effect parameter. To this end, the normalized contact force is defined as

$$F_c(\tau)=1-\left(\frac{1}{\lambda\gamma}\right)^2 \diamond \overline{w}(\xi_M,\tau), \tag{19}$$

the possibility of the moving nanoparticle separation from the surface of ECS could be checked by the sign of the transverse contact force between the moving nanoparticle and the base nanobeam. This phenomenon would be possible when the sign of the transverse contact force changes from positive to negative; however, in the present work, the moving nanoparticle would be in contact with the ECS when it traverses the nanotube structure. To examine the possibility of this phenomenon, the variation of the minimum value of the normalized transverse contact force as a function of moving nanoparticle velocity is depicted in Fig. 7(a)–(c). In the case of without consideration of the inertial effects, the transverse contact force would be equal to the mass weight of the moving nanoparticle. In such a case, $F_c=1$ at all times, regardless of the velocity of the moving nanoparticle (see dashed lines in Fig. 7(a)–(c)). For a moving nanoparticle with an infinitesimal mass weight (say M_N=0.001), the normalized

transverse contact force would be somewhat lower than 1 for different levels of the moving nanoparticle velocity and small scale effect parameter (see Fig. 7(a)). For higher values of mass weight of the moving nanoparticle, the sign of the contact force change from positive to negative for a certain value of moving nanoparticle velocity. A close observation of Fig. 7(b) and (c) reveals that higher values of the small scale effect parameter would generally result in a higher possibility of the moving nanoparticle separation from the SWCNT. Additionally, the absolute value of the minimum transverse contact force commonly increases with the velocity of the moving nanoparticle as well as the small scale effect parameter.

4.2.3. The effect of the mass weight of the moving nanoparticle on the DAFs of displacements and forces of the SWCNT

In Figs. 8 and 9, the variation of DAFs of displacements and internal forces as a function of moving nanoparticle weight is plotted for different values of the small scale effect parameter. The plotted results have been provided for $V_N=0.3$ and four levels of the small scale effect parameter ($e_0a=0$, 0.5, 1, and 1.5 nm). As Fig. 8(a) shows, DAF_u increases with the mass weight of the moving nanoparticle. Moreover, higher small scale effect parameter, higher the predicted value of DAF_u for most values of M_N. As it is seen in Fig. 8(b), the predicted values of DAF_N would lessen as the mass weight of the moving nanoparticle increases. Furthermore, the magnitude of DAF_N increases as the effect of the

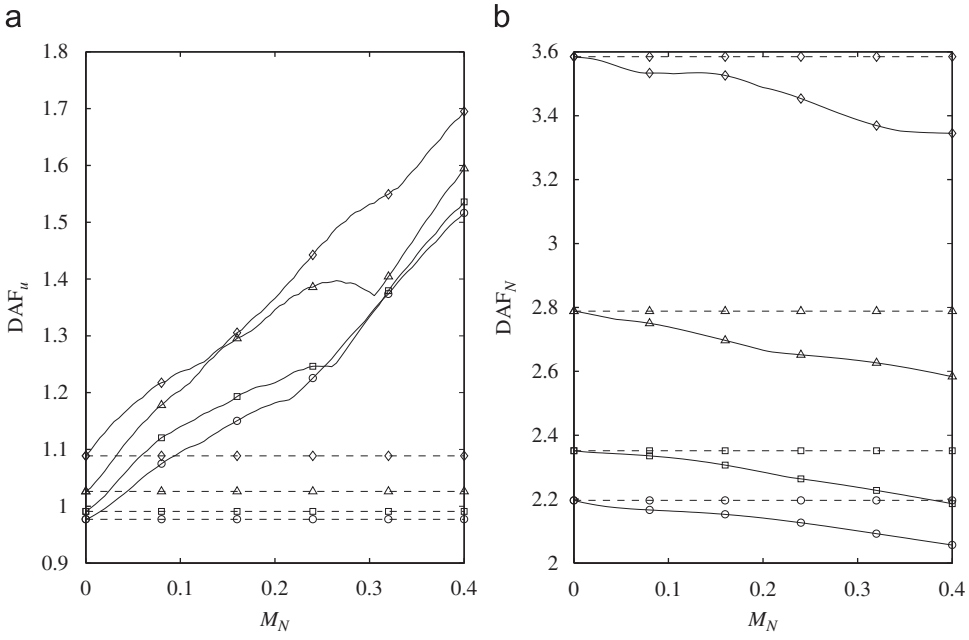

Fig. 8. (a) Plots of DAF_u in terms of M_N and (b) plots of DAF_N in terms of M_N (○ $e_0a=0$ nm; □ $e_0a=0.5$ nm; △ $e_0a=1$ nm; ◇ $e_0a=1.5$ nm; – – – without considering the inertial effects; and (—) by considering the inertial effects; $V_N=0.3$).

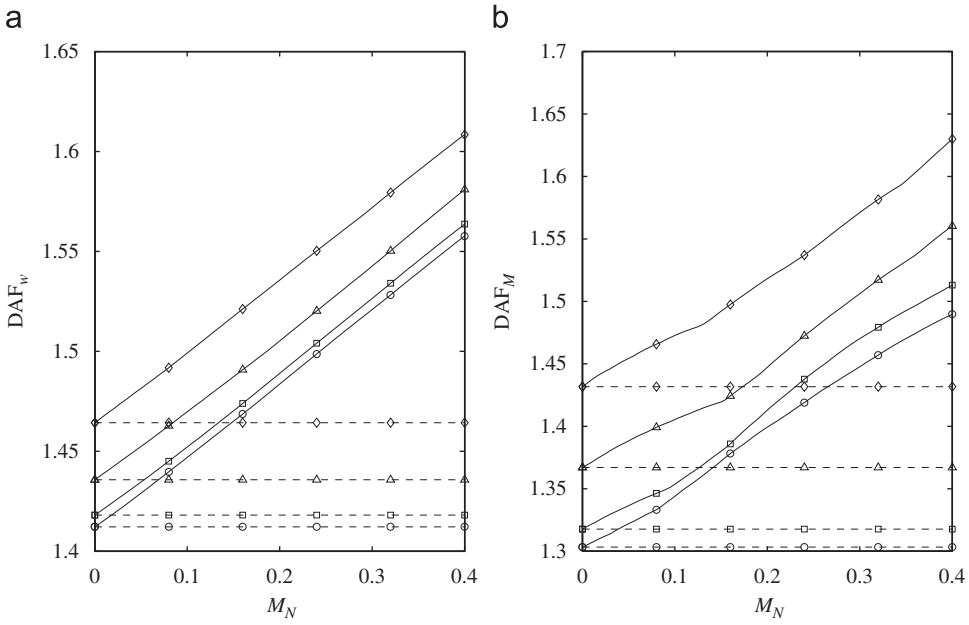

Fig. 9. (a) Plots of DAF_w in terms of M_N and (b) plots of DAF_M in terms of M_N (○ $e_0a=0$ nm; □ $e_0a=0.5$ nm; △ $e_0a=1$ nm; ◇ $e_0a=1.5$ nm; – – – without considering the inertial effects; and (—) by considering the inertial effects; $V_N=0.3$).

small scale parameter becomes highlighted, irrespective of the mass weight of the moving nanoparticle. In Fig. 9(a) and (b), the predicted values of DAF_w and DAF_M are more or less linearly proportional with mass weight of the moving nanoparticle. Moreover, higher small scale effect parameter leads to higher values of DAF_w and DAF_M, regardless of the mass weight of the moving nanoparticle.

4.2.4. The effect of the mass weight of the moving nanoparticle on the minimum and maximum values of the transverse contact force

The plots of the minimum and maximum transverse contact forces as a function of the mass weight of the moving nanoparticle have been provided in Fig. 10(a) and (b) for different levels of the small scale effect parameter. As it is obvious, the minimum transverse contact force decreases with mass weight of the moving nanoparticle; however, the maximum transverse contact force increases with mass weight of the moving nanoparticle. By considering the inertial effect of the moving nanoparticle, the minimum and maximum transverse contact forces generally take lower and higher values, respectively, as the magnitude of small scale effect parameter increases.

4.2.5. The effect of the coefficient of kinetic friction on the DAFs of displacements and forces of the SWCNT

According to the definitions of the DAF_u and DAF_N, it is anticipated that if the longitudinal inertial force of the moving nanoparticle would be negligible in comparison with its frictional force, the obtained values of DAF_u and DAF_N would be fairly independent of the coefficient of kinetic friction. Fortunately, this is the most common case in practical applications of SWCNTs because the longitudinal stiffness of the SWCNTs is commonly much larger than its transverse stiffness. For example, for the under study SWCNT, one could obtain from Eq. (20): $[\overline{\mathbf{K}}_b]_{ij}^{uu}/[\overline{\mathbf{K}}_b]_{ij}^{ww} \approx \lambda^2/(\pi^2 ij) = 41.83^2/(ij)$. This relation implies that the nondimensional longitudinal stiffness of the SWCNT is much larger than the nondimensional transverse stiffness of the SWCNT, particularly for the first modes of vibration, which are the dominant ones. On the other hand, one could arrive at the following relation based on Eq. (20): $[\overline{\mathbf{M}}_b]_{ij}^{uu}/[\overline{\mathbf{M}}_b]_{ij}^{ww} \approx 1$. It is indicated that the predicted transverse displacement would be so larger than the predicted longitudinal displacement. Therefore, the longitudinal inertial force of the moving nanoparticle would be negligible in compare to the transverse inertial force or even the Coulomb frictional force. Moreover, the DAF_w and DAF_M are not affected by the change of the coefficient of kinetic friction because the governing equation in the transverse direction is only expressed in terms of transverse displacement field (see Eq. (4b)). As a result, for a fairly slender SWCNT that the obtained results by the NRBT are trustable, the plotted results of DAF_u, DAF_N, DAF_w, and DAF_M in terms of other parameters remain unchanged for other values of the coefficient of kinetic friction. Furthermore, the presented discussions for those graphs are still valid with a good accuracy, irrespective of the assumed value of coefficient of kinetic friction.

5. Concluding remarks

Dynamic response of a single-walled carbon nanotube (SWCNT) under a moving nanoparticle was scrutinized in the context of the nonlocal continuum theory of Eringen. The equivalent continuum structure (ECS) corresponding to the SWCNT was modeled using nonlocal Rayleigh beam theory under the simply supported boundary conditions. The interaction between the moving nanoparticle and the ECS was taken into account in the modeling of the problem by considering the inertial effect of the moving nanoparticle as well as existing friction between the nanoparticle surface and the inner surface of the ECS. The strong form of the governing equations was established and then the discrete equations of motion were obtained using Galerkin method. The resulting set of ordinary differential equations was solved in the time domain using generalized Newmark-β method. The effects of mass weight of the moving nanoparticle, its velocity, and small scale effect parameter on the dynamic amplitude factors (DAFs) of longitudinal and transverse displacements as well as DAFs of nonlocal axial force and bending moment were studied in some detail. The aforementioned DAFs were extracted in two cases: with and without considering the inertial effects of the moving

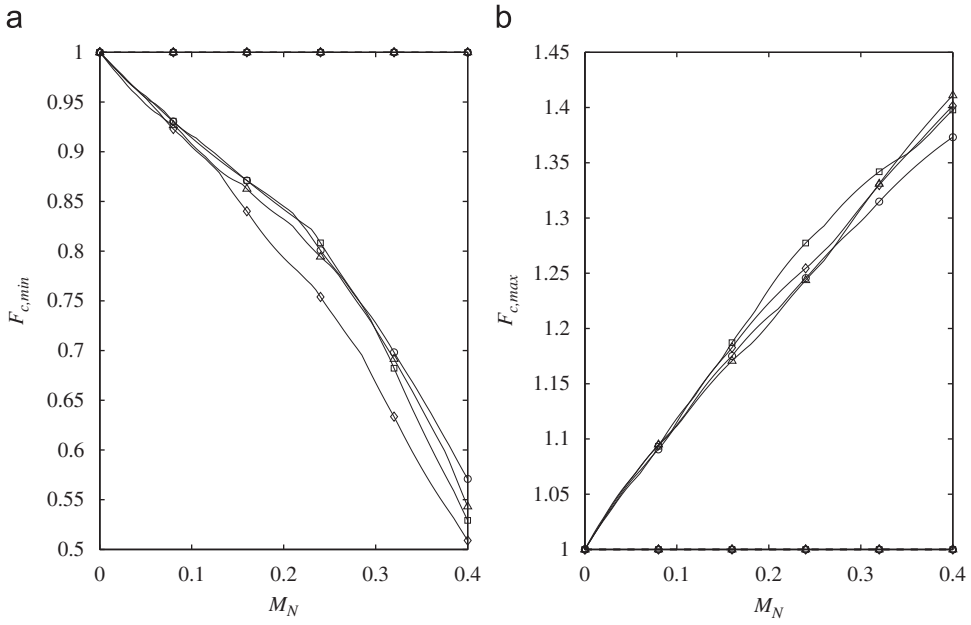

Fig. 10. (a) Plots of $F_{c,\min}$ in terms of M_N and (b) plots of $F_{c,\max}$ in terms of M_N ((○) $e_0a = 0$ nm; (□) $e_0a = 0.5$ nm; (△) $e_0a = 1$ nm; (◇) $e_0a = 1.5$ nm; (– – –) without considering the inertial effects; and (—) by considering the inertial effects; $V_N = 0.3$).

nanoparticle. The obtained results reveal that as the mass weight of the moving nanoparticle increases, not only the differences between the predicted values of DAFs for the above-mentioned cases intensify, but also the predicted values of DAFs of displacements and internal forces would increase. This issue is more obvious when the moving nanoparticle traverses the SWCNT with higher levels of velocity. Furthermore, the predicted DAFs of displacements, axial force, and bending moment generally increase with the small scale effect parameter. The possibility of the moving nanoparticle separation from the inner surface of the SWCNT was also investigated. The possibility of this phenomenon was monitored by the sign of the transverse contact force between the moving nanoparticle and the ECS. The obtained results indicate that the possibility of this phenomenon goes to a greater extent as the mass weight of the moving nanoparticle increases, particularly for higher values of the small scale effect parameter and moving nanoparticle velocity.

Appendix A

For a simply supported ECS with fixed-movable condition, the submatrices in Eq. (11) whose expressions involve integrations are now rewritten in a more simple form as follows:

$$[\overline{\mathbf{M}}_b]_{ij}^{uu} = \Upsilon_{ij}^{uu} + \mu^2 \Gamma_{ij}^{uu} + M_N(\phi_i^u(\xi_M) - \mu^2 \phi_{i,\xi\xi}^u(\xi_M))\phi_j^u(\xi_M) H(1-\xi_M),$$

$$[\overline{\mathbf{M}}_b]_{ij}^{ww} = \Upsilon_{ij}^{ww} + \lambda^{-2}\Gamma_{ij}^{ww} + \mu^2(\Xi_{ij}^{ww} + \lambda^{-2}\Sigma_{ij}^{ww}) + M_N(\phi_i^w(\xi_M) - \mu^2 \phi_{i,\xi\xi}^w(\xi_M))\phi_j^w(\xi_M) H(1-\xi_M),$$

$$[\overline{\mathbf{K}}_b]_{ij}^{uu} = \lambda^2 \Gamma_{ij}^{uu} + M_N(\lambda\beta)^2(\phi_i^u(\xi_M) - \mu^2 \phi_{i,\xi\xi}^u(\xi_M))\phi_{j,\xi\xi}^u(\xi_M) H(1-\xi_M),$$

$$[\overline{\mathbf{K}}_b]_{ij}^{ww} = \Sigma_{ij}^{ww} + M_N(\lambda\beta)^2(\phi_i^w(\xi_M) - \mu^2 \phi_{i,\xi\xi}^w(\xi_M))\phi_{j,\xi\xi}^w(\xi_M) H(1-\xi_M), \tag{A1}$$

where

$$\Upsilon_{ij}^{uu} = \Upsilon_{ij}^{ww} = \begin{cases} 1; & i=j, \\ 0; & i\neq j, \end{cases} \quad \Gamma_{ij}^{uu} = \begin{cases} \pi^2(i-0.5)j; & i=j, \\ 0; & i\neq j, \end{cases}$$

$$\Gamma_{ij}^{ww} = \begin{cases} \pi^2 ij; & i=j, \\ 0; & i\neq j, \end{cases} \quad \Xi_{ij}^{ww} = \begin{cases} \pi^2 i^2; & i=j, \\ 0; & i\neq j, \end{cases} \quad \Sigma_{ij}^{ww} = \begin{cases} \pi^4 i^2 j^2; & i=j, \\ 0; & i\neq j. \end{cases} \tag{A2}$$

References

[1] R.P. Feynman, Eng. Sci. 23 (1960) 22.
[2] S. Iijima, Nature 354 (1991) 56.
[3] A. Bianco, Expert Opin. Drug Discovery 1 (1) (2004) 57.
[4] W. Wu, S. Wieckowski, G. Pastorin, M. Benincasa, C. Klumpp, J.P. Briand, R. Gennaro, M. Prato, A. Bianco, Angew. Chem. Internat. Ed. 44 (39) (2005) 6358.
[5] A. Prokop, J.M. Davidson, J. Pharm. Sci. 97 (9) (2008) 3518.
[6] Y. Rosen, N.M. Elman, Expert Opin. Drug Discovery 6 (5) (2009) 517.
[7] K. Kiani, B. Mehri, J. Sound Vib. 329 (11) (2010) 2241.
[8] K. Kiani, Application of nonlocal beam models to double-walled carbon nanotubes under a moving nanoparticle. Part I: theoretical formulations, Acta Mech. accepted for publication, doi:10.1007/s00707-010-0362-1.
[9] K. Kiani, Application of nonlocal beam models to double-walled carbon nanotubes under a moving nanoparticle. Part II: parametric study, Acta Mech. accepted for publication, doi:10.1007/s00707-010-0363-0.
[10] A.C. Eringen, Nonlocal Continuum Field Theories, Springer-Verlag, New York, 2002.
[11] A.C. Eringen, J. Appl. Phys. 54 (1983) 4703.
[12] L.J. Sudak, J. Appl. Phys. 94 (2003) 7281.
[13] Q. Wang, V.K. Varadan, S.T. Quek, Phys. Lett. A 357 (2006) 130.
[14] T. Murmu, S.C. Pradhan, Physica E 41 (7) (2009) 1232.
[15] H.S. Shen, C.L. Zhang, Compos. Struct. 92 (5) (2010) 1073.
[16] Y.G. Hu, K.M. Liew, Q. Wang, X.Q. He, B.I. Yakobson, J. Mech. Phys. Solids 56 (12) (2008) 3475.
[17] B. Arash, R. Ansari, Physica E 42 (8) (2010) 2058.
[18] L. Wang, H. Hu, Phys. Rev. B 71 (2005) 195412.
[19] J. Yang, L.L. Ke, S. Kitipornchai, Physica E 42 (5) (2010) 1727.
[20] T. Vodenitcharova, L.C. Zhang, Phys. Rev. B 68 (2003) 165401.
[21] A. Pantano, D.M. Parks, M.C. Boyce, J. Mech. Phys. Solids 52 (2004) 789.
[22] S.S. Gupta, R.C. Batra, Comput. Mater. Sci. 43 (2008) 715.
[23] K. Kiani, A. Nikkhoo, B. Mehri, J. Sound Vib. 320 (2009) 632.
[24] H. Heireche, A. Tounsib, A. Benzair, M. Maachou, E.A. Adda Bedia, Physica E 40 (8) (2008) 2791.
[25] M. Ternes, C.P. Lutz, C.F. Hirjibehedin, F.J. Giessibl, A.J. Heinrich, Science 319 (2008) 1066.
[26] Q. Wang, Q.K. Han, B.C. Wen, Adv. Theor. Appl. Mech. 1 (2008) 1.
[27] Q. Wang, C.M. Wang, Nanotechnol. 18 (2007) 075702.
[28] Q. Wang, J. Appl. Phys. 98 (2005) 124301.
[29] M. Aydogdu, Physica E 41 (2009) 1651.
[30] T. Murmu, S.C. Pradhan, Physica E 41 (2009) 1451.